Journal of the European Ceramic Society **18** (1998) 1325–1330

PII: S0955-2219(98)00061-2
0955-2219/98/$—see front matter

Effect of Fluoride on Sinterability of a Silicate Glass Powder

K. Sujirote,[a] R. D. Rawlings[b]* and P. S. Rogers[b]

[a]National Metal and Materials Technology Centre, National Science and Technology Development Agency, Bangkok 10400, Thailand
[b]Department of Materials, Imperial College of Science, Technology and Medicine, London, UK, SW7 2BP

Abstract

Partial substitution of fluorine for oxygen was utilised to increase the crystallisation tendency in glasses based on the Na_2O–CaO–Al_2O_3–SiO_2 system. The glass without fluoride is surface-nucleated and forms wollastonite crystals growing one-dimensionally into the bulk glass. The addition of fluoride facilitates both viscous flow and crystallisation in bulk glass. However, the enhancement of crystallisation due to fluorine can affect processing by the powder route. In the optimum process the glass should sinter to full density before the onset of crystallisation. To achieve this, the relative rates of crystallisation and densification must be optimised by controlling the heating rate. Values of flexural strength as high as 210 MPa can be achieved in fluorine-containing samples of glass-ceramics where both the sintered density and microstructure have been optimised. © *1998 Elsevier Science Limited. All rights reserved*

1 Introduction

Glass–ceramics can be produced either by bulk crystallisation of formed glass products[1,2] or by sintering and crystallisation of pressed glass powders.[3,4] The interest in the sintering of glass arises from the fact that glasses are less prone than ceramics to processing flaws arising from packing defects. For example, large agglomerates can produce flaws in the sintering of ceramics,[5] but glasses usually sinter to full density even when the green microstructure is non-uniform. The theoretical analysis of Boria and Raj[6] suggested that the ability of glass to relax shear stress by viscous flow is the reason why problems of differential sintering are alleviated. The glass route with sintering to near full density, followed by crystallisation, is therefore attractive for making glass–ceramics and glass–ceramic matrix composites.

There are some problems which have to be overcome if a glass powder is to be sintered and heat treated to produce a glass–ceramic. Pre-existing surfaces can act as nucleation sites and the crystallites may grow from the surface of every glass particle towards the centre. Most researchers[7,8] agree that success in producing near full density, high strength materials depends on how far the sintering proceeds before it is halted by crystallisation. Crystallisation of the surface of the vitreous particles may inhibit sintering and consequently pores remain in the product.[9]

Rabinovich[10] found that glass–ceramics which exhibit efficient bulk nucleation may also be difficult to process via a powder route because, on heat treatment, they rapidly develop crystalline phases which inhibit further sintering. It has been further proposed that glasses in which the nucleation of crystal phases is predominantly heterogeneous (i.e. surface rather than bulk nucleated) are more suitable for powder processing because the overall rate of crystallisation is much lower than in materials exhibiting efficient homogeneous nucleation. Therefore in glass–ceramics fabricated by sintering, whether nucleated in the bulk or at the surface, crystallisation must be delayed until sintering is well-advanced if a pore-free, fine and uniform structure is to be obtained. Consequently, the kinetics of sintering and crystallisation plays an important role in determining the sinterability of glass powder to produce glass–ceramics.

The present study concerns the effect of fluoride in bulk and powder samples on the kinetics of

*To whom correspondence should be addressed. Fax: 171 594 6729.

crystallisation and on the ability to sinter glass powders to produce glass–ceramics. The influence of particle size and heating rate on densification kinetics have also been investigated with a view to optimisation of the sintering process.

2 Experimental Procedure

Glasses of compositions shown in Table 1 were prepared from water quenching a silicate melt from 1420°C and then milling in a tungsten carbide Tema mill. Homogeneity was ensured by repeating the melting-quenching-grinding process four times. In order to minimise fluorine volatization, calcium fluoride was introduced in the powder after the third quenching. All powders were dried and sieved mechanically to the required size before being characterised by a Malvern 3600 laser particle size analyser and a JEOL T-220 scanning electron microscope. Two forms of samples were produced, i.e. bulk cast and sintered samples. The bulk cast samples were prepared by casting the fourth melt onto a hot steel plate; the samples were then annealed and underwent various heat treatments. Specimens prepared via the powder route were uniaxially pressed at 1 MPa to the required shape and then were cold isostatically pressed (CIP) at 300 MPa using a Stansted Fluid Power Press. The samples were heat treated at 900, 1000, 1100 and 1200°C.

The crystallisation kinetics were studied using a Phillips PW 1710 X-ray diffractometer and a Stanton Redcroft STA 780 differential thermal analyser. The densification kinetics were investigated using a dilatometer. The mechanical properties were evaluated using three-point bending and single edge notch bending (SENB) techniques in an Instron universal testing machine at a cross-head speed of 0·5 mm min^{-1}.

Table 1. Nominal batch compositions and chemical composition for base glass (CS) and the base glass with substitution of oxygen by fluoride (CSF)

	CS (wt%)	*CSF (wt%)*
Batch composition		
SiO_2	43·45	44·56
Al_2O_3	5·49	5·56
$CaCO_3$	44·4	35·02
Na_2CO_3	6·66	6·85
CaF_2	—	8·01
Chemical composition		
SiO_2	56	54·5
Al_2O_3	7	6·8
CaO	32	24·0
Na_2O	5	4·9
CaF_2	—	9·8
F(from CaF_2)	—	4·8

3 Results and Discussion

3.1 Crystallisation kinetics

In Fig. 1, DTA profiles obtained at a heating rate of 15°C min^{-1} show the typical effects of fluoride addition and morphology of samples. Several thermal events can be observed. The CS bulk glass exhibits one small peak at a temperature of 1135°C whereas the CSF bulk glass shows two exothermic peaks at 864 and 937°C. It can be seen that the addition of fluoride had some significant effects on the crystallisation; substantially lowering the crystallisation temperature to well below the fluoride-free crystallisation temperature and, from the area under the curves which indicates the degree of crystallisation (exothermic reaction), increasing the degree of crystallisation by about 10 times. In addition, results from the X-ray diffractometer (Fig. 2) indicated that the exothermic peak from CS corresponded to the crystallisation of wollastonite ($CaO.SiO_2$) whilst those from CSF corresponded to the initial crystallisation of cuspidine ($CaF_2.3CaO.2SiO_2$) followed by the transformation to wollastonite at a higher temperature ($T > 850$°C).

The DTA profiles of the powdered samples are broadly similar to those obtained from the bulk glasses, i.e. one and two exotherms for CS and CSF glass, respectively. However, several thermal events have been altered by the high surface area of the powdered glasses. Table 2 summarises the isothermal characteristics derived by extrapolation of the DTA data for five finite heating rates to zero rate. It can be seen that the effect of fluoride and

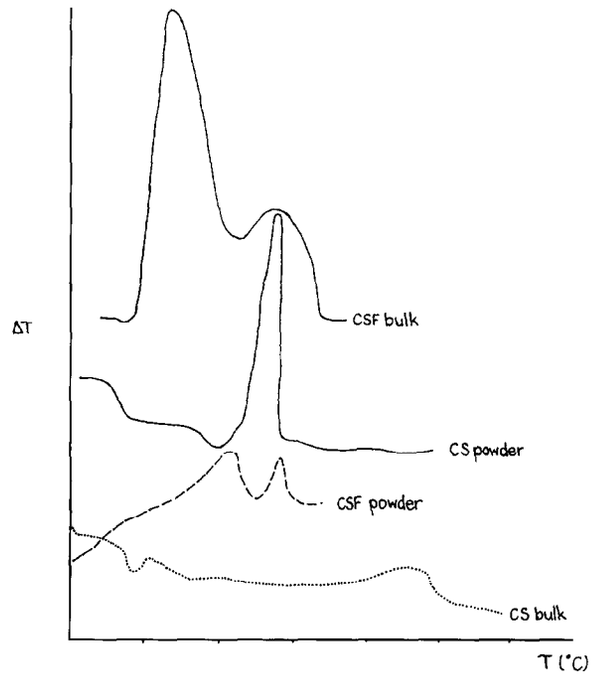

Fig. 1. DTA profiles of CS and CSF bulk and powder samples at 10°C min^{-1}.

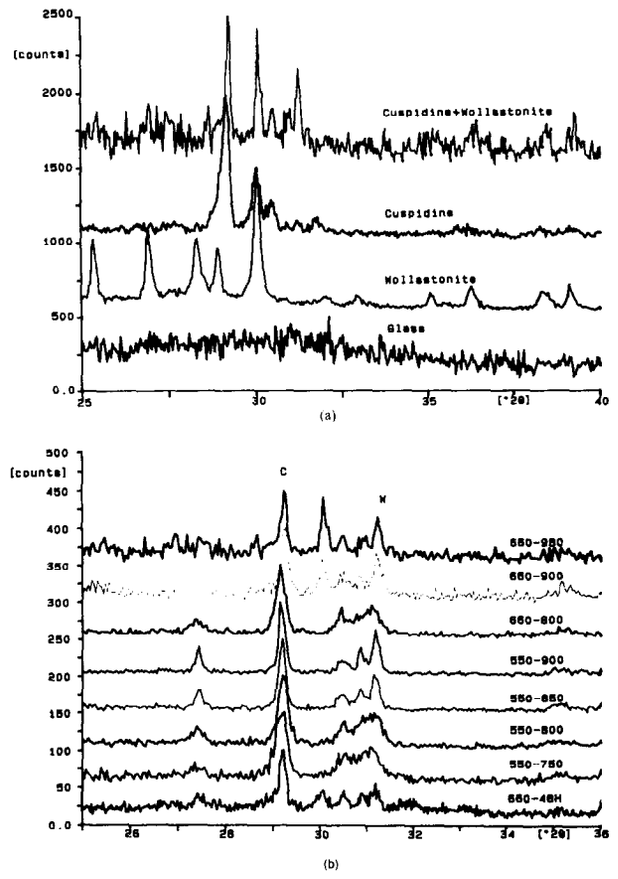

Fig. 2. Typical XRD profiles showing (a) samples with glassy phase, wollastonite, cuspidine, and wollastonite + cuspidine (b) phase transformation from cuspidine to wollastonite.

sample morphology are twofold. Firstly, the sample morphology affects the glass transition temperature, T_g of CS and CSF in opposite directions; the T_g of powder samples is less in CS but slightly greater in CSF with respect to the bulk values. It may be that the presence of free surface facilitates the movement of ions and decreases the viscosity of CS whereas very little influence is seen for CSF.

Secondly, the effect of morphology on T_p–T_x, or the range in which crystallisation started until maximum crystallisation rate is reached, of CS and CSF glasses also occurs in opposite directions. The crystallisation tendency is highly activated in powdered CS glass whereas that of powdered CSF glass appeared to be retarded with respect to the behaviour of the bulk glasses.

Table 2. Isothermal values for glass transition temperature (T_g) and temperature of start and peak of crystallisation (T_x and T_p, respectively), for CS and CSF bulk and powder ($< 38\,\mu m$) samples derived from extrapolation of five heating rates (5, 10, 15, 20, 25, 30°C min^{-1}) to zero heating rate

Thermal characteristics	*Bulk*		*Powder*	
	CS	*CSF*	*CS*	*CSF*
T_g	696	604	676	607
T_x	958	804[a]	834	691[a]
T_p	1108	826[a]	880	748[a]
T_p–T_x	150	22	46	57

[a]Temperatures for first crystallisation peak.

Table 3 shows the activation energy for viscous flow (E_η^*)[11] and for crystallisation (E_c) together with the Avrami exponent.[12] The E_c for bulk CS is close to values for glass forming oxide bond strength[13] or for Ca diffusion in glass.[14] The low value of the Avrami exponent of around unity suggests one dimensional crystal growth. It can be seen that the activation energies for both viscous flow and crystallisation decreased with the presence of free surface in CS glass. Also an unusually high value of 4·9 was obtained for the Avrami exponent for powdered CS. The lower peak crystallisation temperature and activation energies imply that the initiation of crystallisation was markedly accelerated in CS glass powder.

In contrast, the activation energies for bulk CSF glass were similar to that of sodium ion diffusion in glass.[15] The greater mobility of sodium ions in the glass, as compared with Ca^{2+} ions, will lead to greater reactivity of the glass phase and hence higher crystallisability. This is in agreement with the Avrami exponent value of 3 which implies bulk crystallisation. The higher value of E_c and the relatively small decrease in the peak crystallisation temperature for powder CSF suggests that the controlling factor was altered from diffusion of alkali ions to viscous flow and that crystallisation was not enhanced by a large surface area. The low value for the Avrami exponent for the powdered CSF glass is consistent with essentially one-dimensional growth from the surface of each particle.

In summary, the effects of the addition of fluorine on the kinetics of crystallisation are two-fold. Firstly, it increases the number of crystallisation steps by forming a metastable phase, cuspidine. Secondly, it facilitates viscous flow and crystallisation by decreasing the activation energies; it induces crystallisation at lower temperatures and homogeneously in bulk samples. Kinetically speaking the effect of a large area of free surface in powder samples is similar to that of fluorine addition, i.e. the presence of free surface in powdered CS facilitates viscous flow and crystallisation. However, decreasing the CSF particle size leads to

Table 3. Apparent activation energies for viscous flow and crystallisation, and Avrami exponents

Sample	E_η^*(kJ mol^{-1})	E_c(kJ mol^{-1}) T_p	*Avrami exponent*
CS bulk	985	374	0·8
CS < 38 μm	875	354	4·9
CSF bulk	618	132[a]	3·0
CSF < 53 μm	—	278[a]	1·5
CSF < 38 μm	652	308[a]	1·0

[a]Data for first (lower temperature) peak.

an increase in activation energies for viscous flow and crystallisation. Moreover, the mode of crystallisation in CSF powder is surface dominated.

3.2 Densification kinetics

Figure 3 shows the dilatometric plots a 15°C min^{-1} for CS and CSF glass powders. In the early stages of sintering, at temperatures between the glass transition temperature (T_g) and initial sintering temperature (T_{si}), mass transport by surface diffusion should bring about an insignificant overall shrinkage and, at the same time, should decrease the capillary driving force for densification first by increasing the curvature radius of the neck surface between the particles and, next, by coalescence of the particles. The decrease in sample size corresponds to the intermediate stage where the viscosity is greatly decreased and the densification is controlled by viscous flow at the boundary between glass particles. The sudden stop in shrinkage, (at the final sintering temperature, T_{sf}), corresponds to the onset of crystallisation.

It can be seen in Table 4 that T_{si} of CS was approximately 50°C higher than the glass transition temperature. The high temperature 736°C for T_{si} leads to rapid movement of ions in CS. On the other hand sintering commences at around T_g in CSF, i.e. around 609°C. Furthermore in the case of CSF, the onset of crystallisation is at low temperatures ($T_x = 734$°C) giving rise to an abrupt increase of apparent viscosity. As a consequence, sintering was halted and densification was not completed. In contrast CS glass powder sinters and forms a glass monolith before crystallisation commences at 861°C.

3.3 Microstructural development

Figure 4(a) and (b) shows the typical microstructure resulting from crystallisation of cast CS

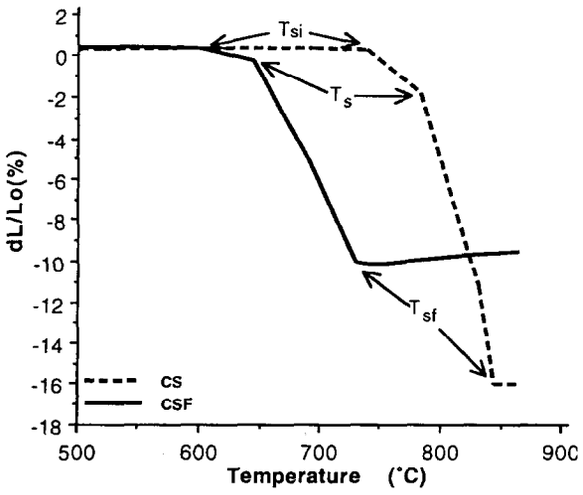

Fig. 3. Dilatometric plots showing effects of temperature on densification of CS and CSF glass powders.

Table 4. Thermal characteristics for CS and CSF (< 38 μm) powders at a heating rate of 15°C min^{-1}

Thermal characteristics (15°C min^{-1})	*Powder*	
	CS	*CSF*
DTA		
Tg	678	609
Tx	861	734
Tp	910	773
Dilatometry		
Tsi	736	600
Ts	781	643
Tf	845	731
Tsi–Tg	48	−9
Tx–Tp	16	3

Glass transition temperatures from DTA (T_g), sintering temperature from dilatometer (T_{si}, T_s and T_{sf}, see Fig. 3) and temperatures of start and peak of crystallisation from DTA (T_x and T_p, respectively).

and CSF glasses, respectively. The micrographs confirmed the results from the kinetics and densification studies. The cast CS glass crystallised one-dimensionally from its surface into the matrix, whilst CSF glass exhibited bulk crystallisation. In the latter the dendritic crystals radiate from nuclei, leading to crystals of spherulite morphology distributed homogeneously in the matrix.

Typical microstructures of CS and CSF glasses obtained via the powder route are shown in Fig. 4(c) and (d), respectively. Sintering in CS proceeded until near-spherical pores were obtained before significant crystallisation could be detected. At 900°C, wollastonite crystals developed in the sintered samples which were very similar to those observed in bulk cast samples except that they were distributed homogeneously in the sintered compact and were smaller. The sintered body was composed of crystals of 10 to 15 μm in length, some residual glass and pores of a few microns in diameter. Increasing the sintering temperature to 1000°C increased the degree of crystallinity.

Observation of the microstructure of CSF sintered compacts revealed much finer crystals and that surface crystallisation predominated. The micrograph shows that crystallisation developed from the surface in each glass particle and severely retarded sintering by preventing viscous flow.

It is interesting to note that a high degree of densification was obtained when the CSF glass compact was sintered at a temperature in the range 850 and 900°C inclusive. The heating rate to reach the sintering temperature was sufficiently fast to ensure that crystallisation was shifted to a high temperature and hence the glass of low viscosity had sufficient time to densify before crystallisation started. At lower sintering temperatures, the viscosity was not low enough and at higher

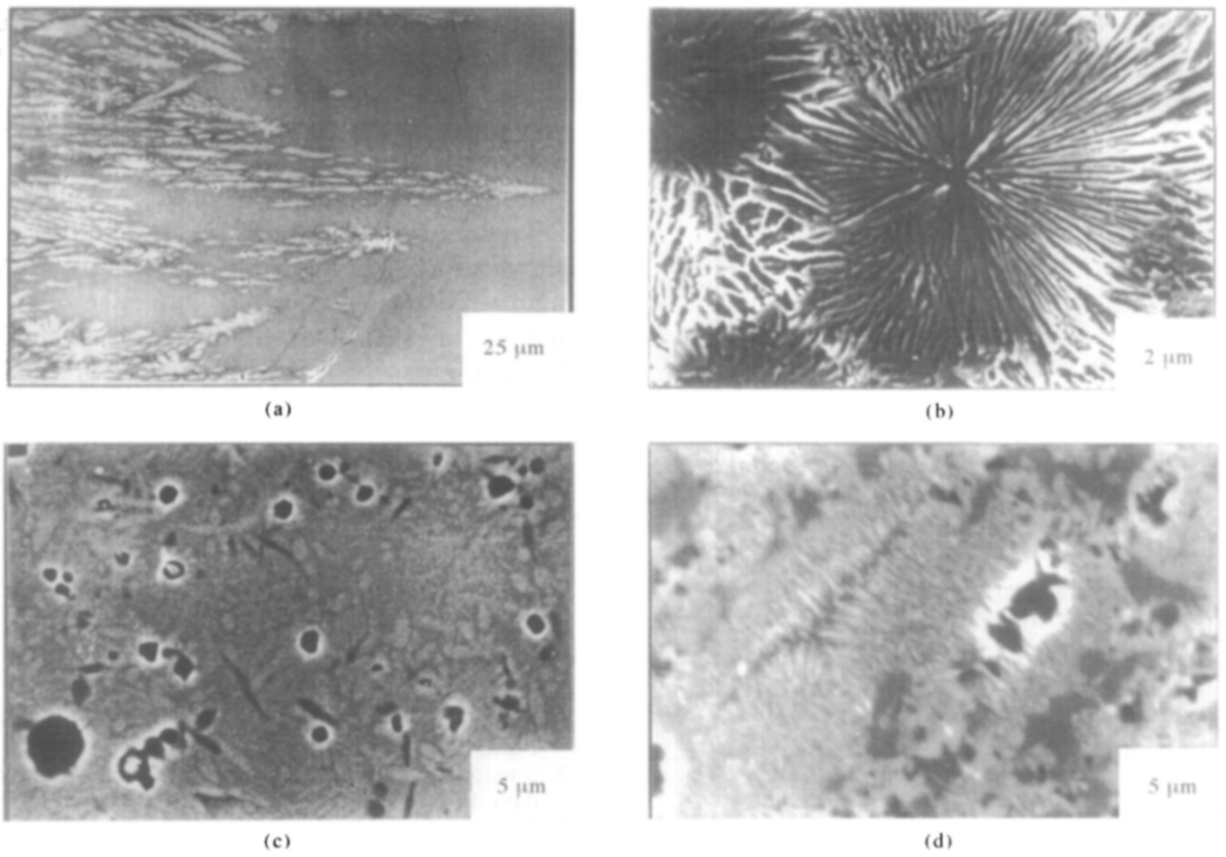

Fig. 4. SEM micrographs of samples heat treated at 900°C (a) CS cast, (b) CSF cast, (c) CS sintered, (d) CSF sintered.

temperatures the crystallisation rate was too high for effective sintering at the heating rates employed.

In summary, it is shown that although the knowledge of crystallisation kinetics in bulk glass is useful, processing via the powder route is complicated by the high surface area of the particles. The main factors controlling the sintering were viscosity and capability for crystallisation. These kinetic and thermodynamic factors can be manipulated by controlling the heating rate and sintering temperature.

3.4 Flexural strength

Heat treatment affected the flexural strength of crystallised CS and CSF samples in different ways. In CS bulk glass, the crystals grow inwards from the glass surface as needles orientated at 90° to the glass surface. When the two 'fronts' of the crystal growth meet a weak interface is formed within the material. Because of the orientation and size of the crystals and the weak interfaces the material has poor mechanical properties (which are not reported).

Figure 5(a) shows the effect of crystallinity of CSF cast samples on the flexural strength. The data have been divided into two curves according to the spherulite morphology, i.e. whether the spherulites were sheaf-like or spherical. The strength dropped with the sheaf-like spherulites because the crystals acted as stress concentration points. As a higher amount of crystallinity developed and the spherulites became spherical, the strength increased until approximately 80% crystallinity was reached. The maximum strength achieved was 154 MPa for 80% crystallised cast CSF from the heat treatment of 900°C for 3 h. At higher degrees of crystallinity, the stress developed at the boundary was so high between the spherulites that microcracks developed and the mechanical strength deteriorated to 100 MPa.

The strength of the sintered samples [Fig. 5(b)] is controlled by heat treatment which directly affects porosity and crystal morphology. In CS glass, the deteriorating effect of the porosity outweighed the small improvement in strength associated with development of a coarse crystal structure. Thus the strength obtained was lower than that of cast glass. Improved strength should be achievable with smaller particle size glass powder and adjusting fabrication parameters, e.g. utilising a slower heating rate and applying pressure during forming and sintering.

The superior strength of CSF on sintering is attributed to the crystals developed being much finer than those in CS samples. The optimal strength value was achieved because the competition between the processes affecting densification, (i.e. sintering and crystallisation), were balanced, giving a low

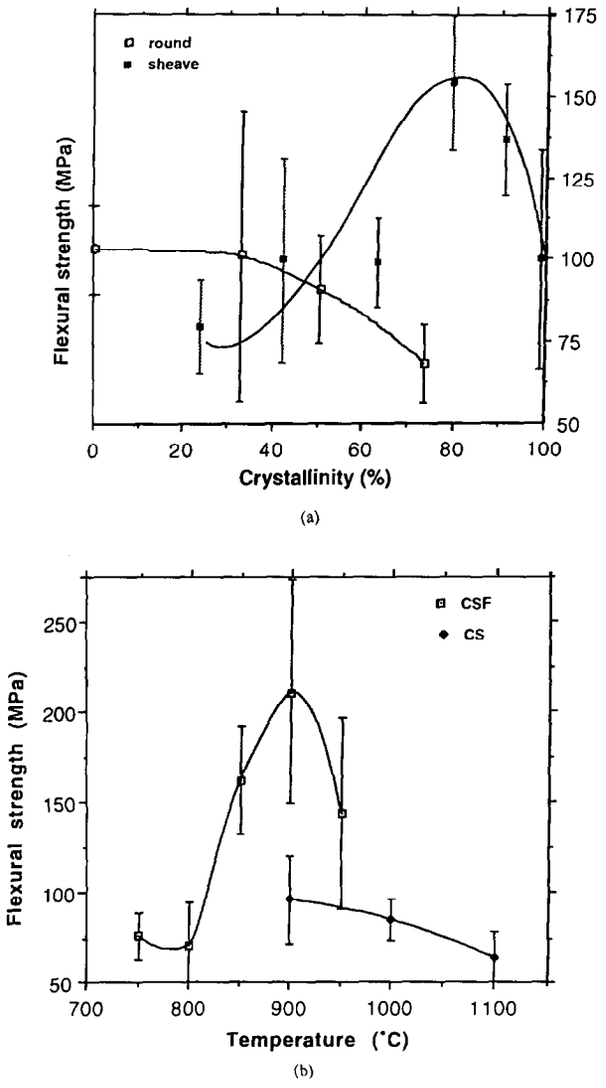

Fig. 5. Effect of (a) crystallinity on flexural strength of samples obtained via bulk route and (b) of heat treatment temperature on flexural strength of samples obtained via powder route.

final porosity and high degree of crystallinity with a small crystal size. The highest flexural strength was 210 MPa and was achieved in samples heat treated at 900°C for 3 h. Lower degree of densification at lower and higher temperature resulted in lower mechanical strength.

4 Conclusion

Viscosity and crystallisation are the predominant controlling factors of glass powder sintering. The addition of fluoride facilitates both viscous flow and crystallisation in bulk glass. However, the enhanced crystallisation tendency of CSF glass, when coupled with the presence of free surface in powdered glasses, has an adverse effect on sinterability. If the crystallisation rate is too high densification is retarded at temperatures above T_g. High density can be achieved only when the CSF compact was sintered at heating rates high enough to allow densification to occur before crystallisation initiated.

Mechanical strength of the cast CSF glass–ceramic material depended on the morphology of the spherulites and the degree of crystallisation. Maximum strength was obtained with spherulite morphology at 80% crystallinity. The strength of glass–ceramics made by sintering CSF and CS glass powders was a function of the porosity, crystal morphology and degree of crystallinity. The highest strength obtained in this study was for CSF glass sintered and crystallised at 900°C for 3 h (210 MPa).

References

1. McMillan, P. W., *Glass–Ceramics*, 2nd edn. Academic Press, London, 1979.
2. Strnad, Z., *Glass–Ceramic Materials*. Elsevier, Amsterdam, 1986.
3. Rabinovich, E. M., Crystallisation and thermal expansion of solder-glass in the $PbO–B_2O_3–ZnO$ system with admixture. *Am. Cer. Soc. Bull.*, 1979, **58**(6), 595–605.
4. Panda, P. C. and Raj, R., Sintering and crystallisation of glass at constant heating rates. *J. Am. Cer. Soc.*, 1989, **72**(8), 1564–1566.
5. Evans, A. G., Considerations of inhomogeneity effects in sintering. *J. Am. Cer. Soc.*, 1982, **65**(10), 497–501.
6. Bordia, R. K. and Raj, R., Analysis of sintering of a composite with a glass or ceramic matrix. *J. Am. Cer. Soc.*, 1986, **69**, C55.
7. Rabinovich, E. M., Cordierite glass–ceramics produced by sintering. In *Advances in Ceramics, Vol. 4, Nucleation and Crystallisation in Glass*, ed. J. H. Simmons, D. R. Uhlmann and G. H. Beall. American Ceramic Society, Westerville, OH, pp. 327–333.
8. Sridharan, S. and Tomozawa, M., Effect of various oxide additives on sintering of $BaO–SiO_2$ system glass–ceramics. *J. Mater. Sci.*, 1992, **27**, 6747–6754.
9. Clark, T. J. and Reed, J. S., Kinetic processes involved in the sintering and crystallisation of glass powders. *J. Am. Cer. Soc.*, 1986, **69**(11), 837–846.
10. Rabinovich, E. M., Review: preparation of glass by sintering. *J. Mater. Sci.*, 1985, **20**, 4259–4297.
11. Moynihan, C. T., Correlation between the width of the glass transition region and the temperature dependence of the viscosity of high T_g glasses. *J. Am. Cer. Soc.*, 1993, **76**(5), 1081–1087.
12. Augis, J. A. and Bennett, J. E., Calculation of the Avrami parameters for heterogeneous solid state reactions using a modification of the Kissinger method. *J. Ther. Anal.*, 1978, **13**(2), 283–292.
13. Sun, K. H., *J. Am. Cer. Soc.*, **30**, 1947, 277–281.
14. Bansal, G. K. and Doremus, R. H., *Handbook of Glass Properties*. Academic Press, London, 1986.
15. Frischat, G. H., Comparison of atom mobility in crystalline and glassy oxides. In *Materials Science Research*, Vol.9, *Mass Transport Phenomena in Ceramics*, ed. A. R. Cooper and A. H. Heuer. Plenum Press, New York, 1975, pp. 285–295.